BBA - Molecular Cell Research 1871 (2024) 119810

Contents lists available at ScienceDirect

BBA - Molecular Cell Research

journal homepage: www.elsevier.com/locate/bbamcr

Research paper

ERK5 mediates pro-tumorigenic phenotype in non-small lung cancer cells induced by PGE2

Arianna Filippelli [a,1], Valerio Ciccone [a,1], Cinzia Del Gaudio [a], Vittoria Simonis [a], Maria Frosini [a], Ignazia Tusa [b], Alessio Menconi [b], Elisabetta Rovida [b,*], Sandra Donnini [a,*]

[a] Department of Life Sciences, University of Siena, 53100 Siena, Italy
[b] Department of Experimental and Clinical Biomedical Sciences "Mario Serio", University of Florence, 50134 Florence, Italy

ARTICLE INFO

Keywords:
Non-small cell lung cancer
Inflammation
PGE2
ERK5
EP receptors
Targeted therapy

ABSTRACT

Lung cancer is the leading cause of cancer-related deaths worldwide, with non-small cell lung cancer (NSCLC) constituting approximately 84 % of all lung cancer cases. The role of inflammation in the initiation and progression of NSCLC tumors has been the focus of extensive research. Among the various inflammatory mediators, prostaglandin E2 (PGE2) plays a pivotal role in promoting the aggressiveness of epithelial tumors through multiple mechanisms, including the stimulation of growth, evasion of apoptosis, invasion, and induction of angiogenesis. The Extracellular signal-Regulated Kinase 5 (ERK5), the last discovered member among conventional mitogen-activated protein kinases (MAPK), is implicated in cancer-associated inflammation. In this study, we explored whether ERK5 is involved in the process of tumorigenesis induced by PGE2. Using A549 and PC9 NSCLC cell lines, we found that PGE2 triggers the activation of ERK5 via the EP1 receptor. Moreover, both genetic and pharmacological inhibition of ERK5 reduced PGE2-induced proliferation, migration, invasion and stemness of A549 and PC9 cells, indicating that ERK5 plays a critical role in PGE2-induced tumorigenesis. In summary, our study underscores the pivotal role of the PGE2/EP1/ERK5 axis in driving the malignancy of NSCLC cells in vitro. Targeting this axis holds promise as a potential avenue for developing novel therapeutic strategies aimed at controlling the advancement of NSCLC.

1. Introduction

Lung cancer stands as the primary contributor to global cancer-related mortality. Non-small cell lung cancer (NSCLC) comprises about 85 % of all lung cancers. Despite progress in early detection and various aspects of treatment, the survival rate for lung cancer patients remains low. While active and passive smoking exposure is the primary risk factor for lung cancer, other risk factors like occupational hazards, environmental exposures, and pre-existing lung conditions characterized by persistent inflammation, such as chronic obstructive pulmonary disease and idiopathic pulmonary fibrosis, also play a significant role for this type of cancer [1].

Inflammation is a key player throughout different phases of lung tumor development, influencing its initiation, promotion, invasion and metastasis. These processes intricately influence immune surveillance, as well as responses to therapy [2,3]. Prostaglandin E2 (PGE2), a derivative of the cyclooxygenase-2 (COX-2) pathway, is secreted by both tumor cells and nearby stromal cells. Elevated PGE2 levels emerge as a recurring theme across a diverse spectrum of human tumors [4]. PGE2 in the tumor microenvironment drives various aspects of tumor progression, including invasion, evading programmed cell death, adopting a mesenchymal state, and acquiring stem cell-like properties [5,6]. Additionally, it boosts angiogenesis while suppressing the immune surveillance anti-tumor defenses [7]. Research suggests that COX-2 inhibitors could have a promising role in treating advanced cancers, including NSCLC [8]. Although many preclinical, epidemiological, and clinical studies have reported the existence of a strong association between PGE2 and the development or progression of cancer, the underlying molecular mechanisms remain unclear. PGE2 influences target cells in an autocrine or paracrine manner, activating downstream signals via specific G protein-coupled receptors known as EP1, EP2, EP3, and EP4 [9]. Furthermore, it has been observed that PGE2-activated EP receptors may utilize receptor tyrosine kinases to transmit their signals [10,11]. Among the signal transduction pathways, the mitogen-

* Corresponding authors.
E-mail addresses: elisabetta.rovida@unifi.it (E. Rovida), sandra.donnini@unisi.it (S. Donnini).
[1] These authors contributed equally to this work.

https://doi.org/10.1016/j.bbamcr.2024.119810
Received 24 January 2024; Received in revised form 25 July 2024; Accepted 4 August 2024
Available online 10 August 2024

activated protein kinase (MAPK) family, particularly the Extracellular signal-Regulated Kinase1/2 (ERK1/2) is critical in the cancer-promoting functions of PGE2 [12].

Another member of the MAPK family is ERK5, also referred to as Big Mitogen-activated protein Kinase 1 (BMK-1), which is a key signaling molecule involved in a wide array of cellular processes, ranging from cell division, differentiation and survival to migration [13,14]. ERK5 activation is reached through MEK5-dependent or -independent phosphorylation that stimulates ERK5 nuclear translocation, a key event for cell proliferation [13,15]. Structurally, ERK5 is featured by an N-terminal region, which contains the kinase domain, and a C-terminal extension, unusually long, able to modulate ERK5 subcellular distribution and endowed with transcriptional co-activator function. In the inactive form, ERK5 assumes a closed conformation, where the binding between N- and C-terminal blocks its catalytic activity. In the inactive form ERK5 is stabilized and anchored into the cytosol by HSP90 and CDC37. The catalytic activity of ERK5 is stimulated by the dual phosphorylation of its regulatory Thr-Glu-Tyr (TEY) motif, operated by MEK5, followed by the autophosphorylation of its C-terminal tail, at several Ser and Thr residues. Finally, the open conformation of active ERK5, detached from HSP90, is able to dynamically shuttle between the cytosol and the nucleus [13,16,17] via Beta1 importin [18].

ERK5 activation has been associated with the onset and progression of several types of cancers, such as lung, breast, colorectal, prostate, and pancreatic cancers [14,16,17]. In particular, the deregulation of MEK5/ERK5 pathway plays a multifaceted role in tumor development and progression, fostering uncontrolled cell growth, regulating angiogenesis and epithelial-mesenchymal transition and even contributing to therapy resistance in certain cancers [19,20]. ERK5 is also implicated in cancer-associated inflammation [21]. For instance, inhibition of ERK5 in macrophages induces a transcriptional switch that blocked protumor macrophage polarization [22]. In the context of epidermal carcinogenesis, ERK5 is involved in controlling the expression of a subset of proinflammatory cytokines, and inhibition of ERK5 suppressed inflammation-driven tumorigenesis [23].

While there are numerous studies that demonstrate the involvement of PGE2 and ERK5 in tumorigenesis individually, direct evidence specifically linking PGE2 with ERK5 in tumors is lacking. This research delves into the interplay between PGE2 and ERK5 in the regulation of a pro-tumorigenic phenotype in two models of NSCLC cells, A549 and PC9. Here, we demonstrate that PGE2 induces ERK5 activation through EP1 receptor, and that ERK5 knockdown or pharmacological inhibition with XMD8-92 [24] significantly curbs PGE2/EP1-driven growth, invasion, and stemness of NSCLC cell lines.

2. Materials and methods

2.1. Reagents

PGE2 was solubilized in ethanol (10 mM) (Sigma Aldrich, St. Louis, MO, USA). ERK5 inhibitor XMD8-92 was from Santa Cruz (Heidelberg, Germany) and dissolved in DMSO (10 mM). Recombinant human EGF was supplied by PeproTech (Rocky Hill, NJ, USA). EP receptors agonists 17-phenyl trinor Prostaglandin E2 ethyl amide as EP1 agonist, Butaprost as EP2 agonist, Sulprostone as EP3 agonist, and L-902,688 as EP4 agonist were provided by Cayman Chemical (Ann Arbor, MI, USA).

Lentiviral particles used to achieve a stable knockdown of target genes were provided by OriGene Technologies (Rockville, MD, USA). The kit for fast staining (fast Panoptic) was from PanReac AppliChem ITW Reagents (Darmstadt, Germany).

DMSO, CelLytic MT Cell Lysis Reagent, TWEEN 20 and Phosphate Buffered Saline (PBS) were provided by Merck KGaA (Darmstadt, Germany).

2.2. Cell cultures

A549 human lung cancer cell line (passages 12–20, CCL-185) was purchased from American Type Culture Collection (ATCC); PC9 human lung cancer cells (passages 12–20, 90071810) were purchased from European Collection of Authenticated Cell Cultures (ECACC). All the cell lines were cultured in Dulbecco's Modified Eagle Medium (DMEM) 4500 high glucose supplemented with 10 % heat-inactivated foetal bovine serum (FBS), 2 mM L-glutamine and 100 U/ml penicillin and 100 μg/ml streptomycin (Merck KGaA, Darmstadt, Germany) and maintained in a humidified incubator with 5 % CO_2 at 37 °C. Cells were propagated by splitting 1:4 twice a week for A549 and 1:3 twice a week for PC9.

To stably downregulate ERK5 (encoded by the *MAPK7* gene) in A549 human shRNA lentiviral transduction particles were purchased from Merck KGaA (Darmstadt, Germany; clones: TRCN0000010275 and TRCN0000197264). For viral infections, cells were incubated for 24 h with viral particles at 10 MOI in the presence of 8 μg/ml polybrene. Transduced cells were selected with 2 μg/ml puromycin for at least 72 h. ERK5 protein expression was assessed by multiple and periodical Western Blot analysis. Cells were expanded and used until 20 passages.

2.3. Proliferation assay

1×10^3 cells/well (of a 96-well multiplate) were grown in adhesion in 10 % FBS for 24 h and then treated with PGE2 [0.1–1 μM], EGF [25 ng/ml] and XMD8-92 [5 μM for A549 and 2.5 μM for PC9] in low serum concentration (1 % FBS). High serum concentration was used as positive control (10 % FBS). All experimental points were run in triplicate. After 24 and 48 h, cells were fixed using Fixing for fast staining (methanol based) (Panoptic No. 1) for 15 min at room temperature and then stained using Eosin for fast staining (Panoptic No. 2) and Blue for fast staining (Panoptic No. 3; Azur B based; 15 min each; PanReac AppliChem). Cells were randomly counted at 20× original magnification in 5 fields by using Nikon Eclipse E400 [25]. Data are reported as the mean of cells counted/well.

2.4. Cell cycle analysis

Cell cycle distribution was analyzed using flow cytometry after propidium iodide staining. NSCLC (7×10^5 cells/well) were seeded in 6-multiwell plates in growth medium with 10 % FBS for 24 h, left overnight to allow for cell attachment, and then exposed to 1 % FBS for 24 h and then treated with PGE2 (1 μM), XMD8-92 (5 μM, 30 min pretreatment) with/without EGF (25 ng/ml) for 24 h. Cells were then washed three times with PBS, trypsinized and collected by centrifugation at 0.3 ×*g* for 5 min. The cells were fixed overnight in 70 % ethanol at −20 °C, then washed twice with PBS and incubated with 0.5 ml of PBS containing 100 μg/ml RNase Merck KGaA (Darmstadt, Germany) and 50 μg/ml propidium iodide [Merck KGaA (Darmstadt, Germany)] at 37 °C for 30 min. Samples were read with a FACSCalibur TM cytofluorimeter with CELLQuest software version 3.3. The excitation of PI was made with an argon-ion laser at 488 nm, and PI emission was recorded with FL2 (filter 585/42 nm, detection range 564–606 nm). A 10,000 total events per sample were acquired [26].

2.5. Western blot

Sub-confluent cells were serum starved for 18 h. Cells were then exposed to fresh media added with 1 % FBS. To evaluate the activation of ERK5, cells were treated with increasing concentrations of PGE2 [0.1–1 μM] for 15 min. Treatment with EGF [25 ng/ml] was performed for 10 min, as a positive control of ERK5 activation. Treatment with EP1, EP2, EP3 and EP4 agonists was performed for 15 min (1 μM). Protein extraction and Western Blot were performed as previously described [27]. Briefly, 50 to 100 μg of proteins for each sample were subjected to electrophoresis in 4–12 % Bis-Tris Gels (Life Technologies, Carlsbad, CA,

USA). To evaluate stemness markers, 50 μg of proteins extracted from tumorspheres (see below) were used.

Proteins were blotted onto nitrocellulose membranes and then incubated overnight at 4 °C with primary antibodies: anti-pERK5 (Thr218/Tyr220; #3371), anti-ERK5 (#3372), anti-β-actin (#3700), anti-KLF4 (#4038), anti-OCT4 (#2840), anti-SOX2 (#2748), anti-NANOG (#4903), anti-cMYC (#5605), anti-KLF2 (#51221), anti-p90RSK (Ser380; #9341), anti-pSGK1 (Ser78; #5599), GAPDH (#5174) were provided by Cell Signaling Technology (Danvers, MA, USA); Tubulin (T8203), provided by Merck KGaA, Darmstadt, Germania; anti-pERK5 (Ser496; orb5183) provided by Biorbyt (Durham, NC, USA). The molecular weight marker, Dual Color Standards, was provided by Biorad (Hercules, CA, USA).

The detection was carried out by enhanced chemiluminescence system (Biorad, Hercules, CA, USA), or by infrared imaging using an Odyssey detector (Licor, Lincoln, NE, USA) as previously described [28]. For each sample the arbitrary densitometry unit (ADU) was calculated by Fiji software (64-bit Java 1.8.0_172). Data were normalized on β-actin and presented as means ± SD of at least three experiments. Protein loading was performed on the same membranes or on the same lysates.

2.6. Tumor cell migration

To assess the migration of adherent cells treated with PGE2 [0.1–1 μM], scratch assay was performed as previously described [29]. NSCLC cells (2×10^5 cells/well) were seeded in 24 multiwell plates in medium with 10 % FBS, up to a confluent state. A scratch was mechanically performed on the layer of cells, then treated with increasing concentrations of PGE2 [0.1–1 μM] or XMD8-92 [2.5 μM for PC9 and 5 μM for A549] diluted in medium added with 1 % FBS. The antimitotic compound cytosine arabinoside (ARA-C) [2.5 μg/ml] was added in all the wells. Images of the wound in each well were acquired from 0 to 18 h under a phase contrast microscope (Nikon Eclipse TE 300, Nikon, Tokyo, Japan), at 10× magnification. The rate of migration was calculated by quantifying the area of wound at the starting time and after 18 h. Results (mean ± SD) are expressed as percentage of area of wound respect to time to control (untreated cells).

2.7. Tumor cell invasion

To evaluate cell invasiveness, NSCLC cells were exposed to PGE2 [0.1–1 μM] or EGF [25 ng/ml]. The Neuro Probe 48-well microchemotaxis chamber (Nuclepore Corp., Pleasanton, CA, USA) was used. Polyvinylpyrrolidone (PVP)-free polycarbonate filters, 8 μm pore size were coated with gelatin 1 % (Gelatin from bovine skin, type 1, Sigma Aldrich, St. Louis, MO, USA) [30]. 50 μL of cell suspension (2.5×10^4 cells/mL) were added to each upper well. Before seeding, tumor cell suspensions were treated with PGE2 [0.1–1 μM], EGF [25 ng/ml], XMD8-92 [5 μM for A549 and 2.5 μM for PC9] or EP receptors agonists [1 μM]. Once assembled, the chamber was incubated at 37 °C for 8 h. Then, the filter was removed and fixed in methanol overnight. Cells were stained, and the filter mounted on glass coverslips. Migrated cells were counted using a light microscope (Nikon Eclipse E400 at 20× magnification) in 5 random fields per each well. Cell migration was measured by the number of cells moving across the filter. Each experimental point was done in triplicate and was presented as mean value of migrated cells (±SD).

2.8. Clonogenic assay

5×10^2 cells/well were seeded into 6-well plates and incubated in medium supplemented with 1 % FBS for 18 h. Then, cells were treated in triplicates with PGE2 [0.1–1 μM] or EGF [25 ng/ml] with or without XMD8-92 [5 μM for A549], in 1 % FBS medium. 10 days after treatment, cells were fixed and stained with Panreac kit (Darmstadt, Germany), and colonies (>50 cells) were counted. Data are reported as mean of counted colonies (±SD) [31].

2.9. In vitro tumorsphere formation assay

To assess the ability of single cells to generate tumorspheres, the in vitro surrogate of stem-like cells, 2×10^5 cells/well were distributed into an ultralow-attachment 6-well plate [32]. All tumorspheres were grown in DMEM-F12 medium (Gibco, Milan, Italy), supplemented with penicillin/streptomycin, L-glutamine, and allowed to grow for 7 days, or until the majority of spheres reached a diameter of 60 μm. Tumorspheres were treated with PGE2 [0.1–1 μM] or EGF [25 ng/ml], once a day, and XMD8-92 [2.5 μM for PC9 and 5 μM for A549], added every 48 h. Tumorspheres were counted and then harvested followed by protein extraction or split for second and third tumorsphere generation and lysed for protein extraction.

2.10. Immunofluorescence analysis

The nuclear translocation of β-catenin was visualized in A549SC and A549KD by immunofluorescence analysis. 3×10^4 cells were seeded on 1 cm glass coverslips added in the bottom of a 24 well multiplate. After 24 h of incubation, cells were treated with PGE2 [1 μM] for 4 h. Immunofluorescence analysis was performed as previously reported [33] using anti β-catenin antibody (#8480, Cell Signaling Technology), and DAPI as nuclear counterstaining dye. Images were taken using a confocal microscope (Zeiss LSM700; Zeiss GmbH, Oberkochen, Germany).

2.11. RNA isolation and quantitative RT-PCR

Sub-confluent cells were serum starved for 18 h. Cells were then exposed to fresh media, added with 1 % FBS. To evaluate the activation of ERK5, cells were treated with increasing concentration of PGE2 [0.1–1 μM] for 24 h.

Total RNA was prepared using a RNeasy Plus Kit (#74134 Qiagen, Milan, Italy) following the manufacturer's instructions. One microgram of RNA was reverse-transcribed using QuantiTect Reverse Transcription Kit (#205313 Qiagen), and quantitative RT-PCR (QPCR) was performed using QuantiNova SYBR Green PCR Kit (#208056 Qiagen) in a Rotor-Gene Q PCR machine (Qiagen). Fold change expression was determined by the comparative Ct method (ΔΔCt) normalized to GAPDH [34]. The primers sequences (Merck KGaA, Darmstadt, Germany) were: EP1 forward:

5′-GGTATCATGGTGGTGTCGTG-3′ and reverse: 3′-CGCTGCAGGGAGGTAGAG-5′. EP2 forward: 5′-GGAAGTCAATATGTGGAAGCAA and reverse: 3′-CGAAGAGCATGAGCATCGT-5′. EP3 forward: 5′-AACCAGATCTTGGATCCTTGG-3′ and reverse: 3′-TCTCCGTGTGTGTCTTGCAG-5′. EP4 forward: 5′-ACAAGGTATAATAAAATTATCGCAACC-3′ and reverse: 3′-CATCTGCAACTTCAGCTGGTTA-5′. C-Myc forward: 5′-CACCAGCAGCGACTCTGA-3′ and reverse: 3′-CCTGTGAGGAGGTTTGCTGTG-5′. GAPDH forward: 5′-CAATGGAGAAGGCTGGGG-3′ and reverse: 3′-CAAAGTTGTCATGGATGACC-5′.

2.12. Statistical analysis

The results (mean ± SD) were derived from at least three independent experiments, each performed in triplicate. A one-way ANOVA followed by Bonferroni's post hoc test was selected for statistical analysis by using Microsoft Excel. p-value <0.05 indicates statistical significance.

3. Results

3.1. PGE2 activates ERK5 in NSCLC cells through EP1 receptor

To establish whether ERK5 plays a role in PGE2-mediated NSCLC cell

growth and invasion, we used two NSCLC cell lines, A549 and PC9, expressing basal levels of ERK5 (Fig. 1A). In A549 and PC9 cells, ERK5 presented as a doublet, in which the upper band corresponds to the extensively phosphorylated and active form, in line with previous reports [35,36]. In A549 cells, a loss-of-function approach was also used. Briefly, A549 were appropriately transfected with lentiviral vectors carrying control shRNA encoding for a scrambled sequence (SC) or two different ERK5-specific shRNAs (KD A or B) (Fig. 1A). Each ERK5KD was validated for ERK5 expression by Western Blot. Gene silencing with both ERK5-specific shRNAs efficaciously reduced basal expression levels of ERK5 (Fig. 1A). Then, we explored the ability of PGE2 to activate ERK5 in NSCLC cells. PGE2 promoted ERK5 activation in A549 cells (Fig. 1B) with a marked effect at 1 μM, as witnessed by the increased amount of the upshifted band in Western Blot analysis. EGF, a well know upstream activator of ERK5, was used as a positive control [37]. Similarly, in PC9 cells, PGE2 (1 μM) promoted ERK5 activation, with a response of comparable magnitude to that promoted by EGF (Fig. 1C).

In light of these results, we investigated the receptor subtype involved in PGE2-induced ERK5 activation. First, we analyzed the expression of EP receptor subtypes in the NSCLC cell lines employed in

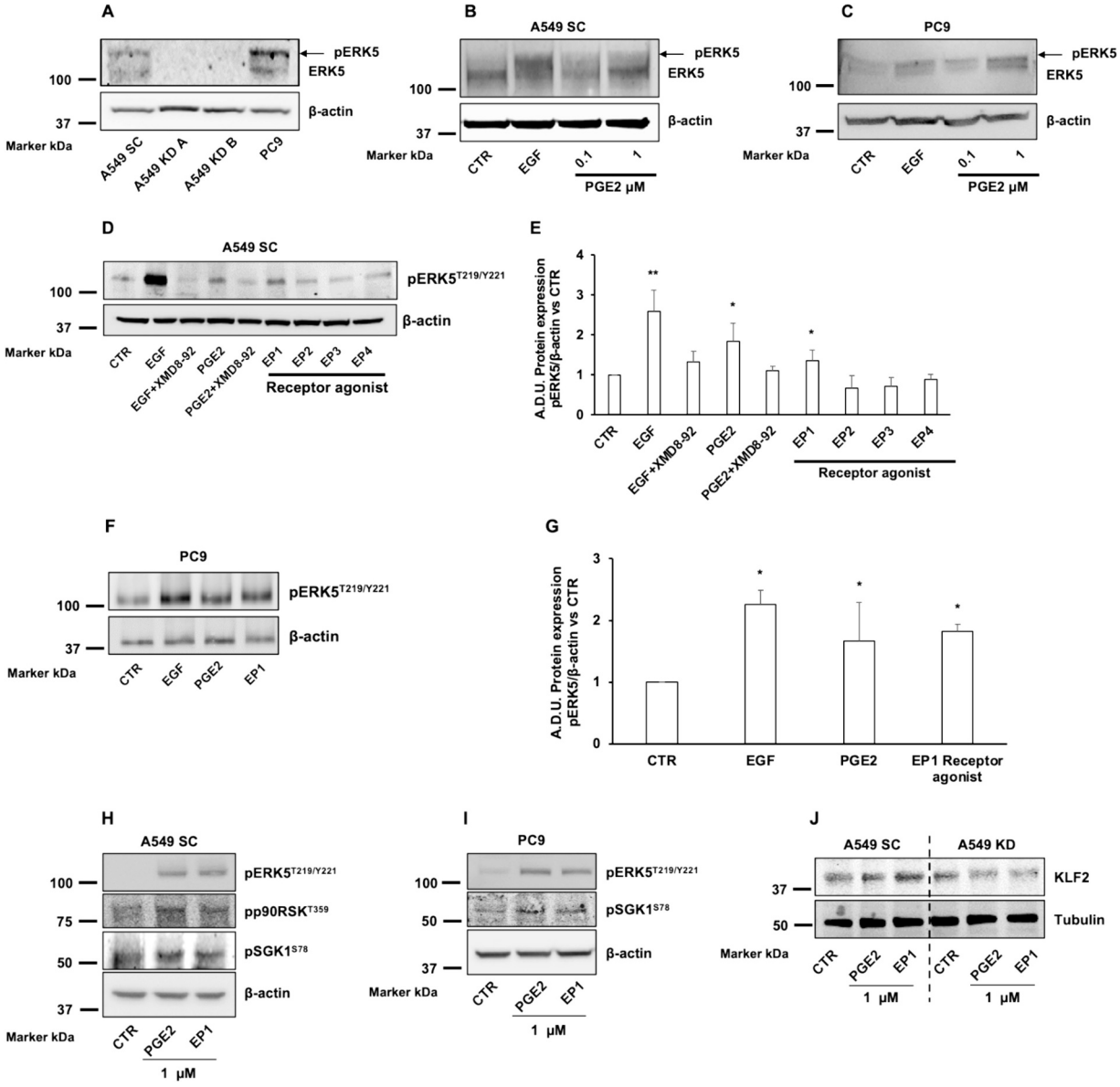

Fig. 1. PGE2 and EP1 stimulation activates ERK5 in NSCLC cells. (A–C). Basal expression of ERK5 (115 kDa) in A549 cells transfected with lentiviral vectors carrying control shRNA encoding for a scrambled sequence (SC) or ERK5-specific shRNA (KD A or B) and in PC9 cells after 48 h of growth in 10 % FBS (A). ERK5 activation (115 kDa) in A549 SC (B) and PC9 (C) cells exposed to EGF (25 ng/ml, 15 min) or PGE2 (0.1 and 1 μM for 15 min). β-actin (45 kDa) was used as loading control. Blots are representatives of three independent experiments. Hyperphosphorylated ERK5 upshifted band is indicated by an arrow. (D). ERK5 phosphorylation (115 kDa) levels in A549 SC cells exposed to EGF (25 ng/ml), PGE2 (1 μM) with/without XMD8-92 (5 μM, 30 min pretreatment), or PGE2 receptor agonists (1 μM) for 15 min. (E). Quantification of blots reported in (D). CTR condition has assigned 1. *$p < 0.05$ and **$p < 0.01$ vs CTR. β-actin (45 kDa) was used as loading control. Blots are representatives of three independent experiments. (F). ERK5 phosphorylation (115 kDa) levels in PC9 cells exposed to EGF (25 ng/ml), PGE2 (1 μM), EP1 receptor agonist (17-phenyl trinor Prostaglandin E2 ethyl amide) (1 μM) or EGF (25 ng/ml) for 15 min. (G). Quantification of blots reported in (F). CTR condition has assigned 1. *$p < 0.05$ vs CTR. β-actin was used as loading control. Blots are representatives of three independent experiments. (H). Phosphorylation levels of ERK5 (T219/Y221) (115 kDa), p90RSK (T379) (90 kDa), and SGK (S78) (54 kDa) in A549 SC cells exposed to PGE2 (1 μM) or EP1 receptor agonist (1 μM) for 15 min. (I). Phosphorylation levels of ERK5 (T219/Y221) (115 kDa) and SGK (S78) (54 kDa) in PC9 cells exposed to PGE2 (1 μM) or EP1 receptor agonist (1 μM) for 15 min. (J). KLF2 expression (42 kDa) levels in A549 SC and KD exposed to PGE2 (1 μM) and EP1 (1 μM) for 60 min. Molecular weight markers on the left of blots.

this study. We observed that mRNA for all four receptors were expressed in roughly equal amounts in all cell lines used, regardless of ERK5 expression (Supplementary Fig. 1). Therefore, we examined whether agonists of the individual receptor subtype were able to activate ERK5 by Western Blot analysis. To this end, we used specific EP receptor agonists at 1 μM for 15 min: 17-phenyl trinor Prostaglandin E2 ethyl amide as EP1 agonist, Butaprost as EP2 agonist, Sulprostone as EP3 agonist, and L-902,688 as EP4 agonist. In A549, EGF, used as positive control, promoted a significant (over 2-fold higher than baseline) ERK5 activation. Both PGE2 and EP1 agonists showed a significant ERK5 activation (Fig. 1D, E). As expected, XMD8-92, a pharmacological ERK5 inhibitor, reverted PGE2-induced activation of ERK5 in A549, as witnessed by the reduced phosphorylation at ERK5 [38]. We found the same results in PC9, where PGE2 and EP1 receptor agonist promoted ERK5 activation (almost 1.7-fold more than in untreated cells) (Fig. 1F, G).

Activation of ERK5 by PGE2 and EP1 (1 μM) was further confirmed

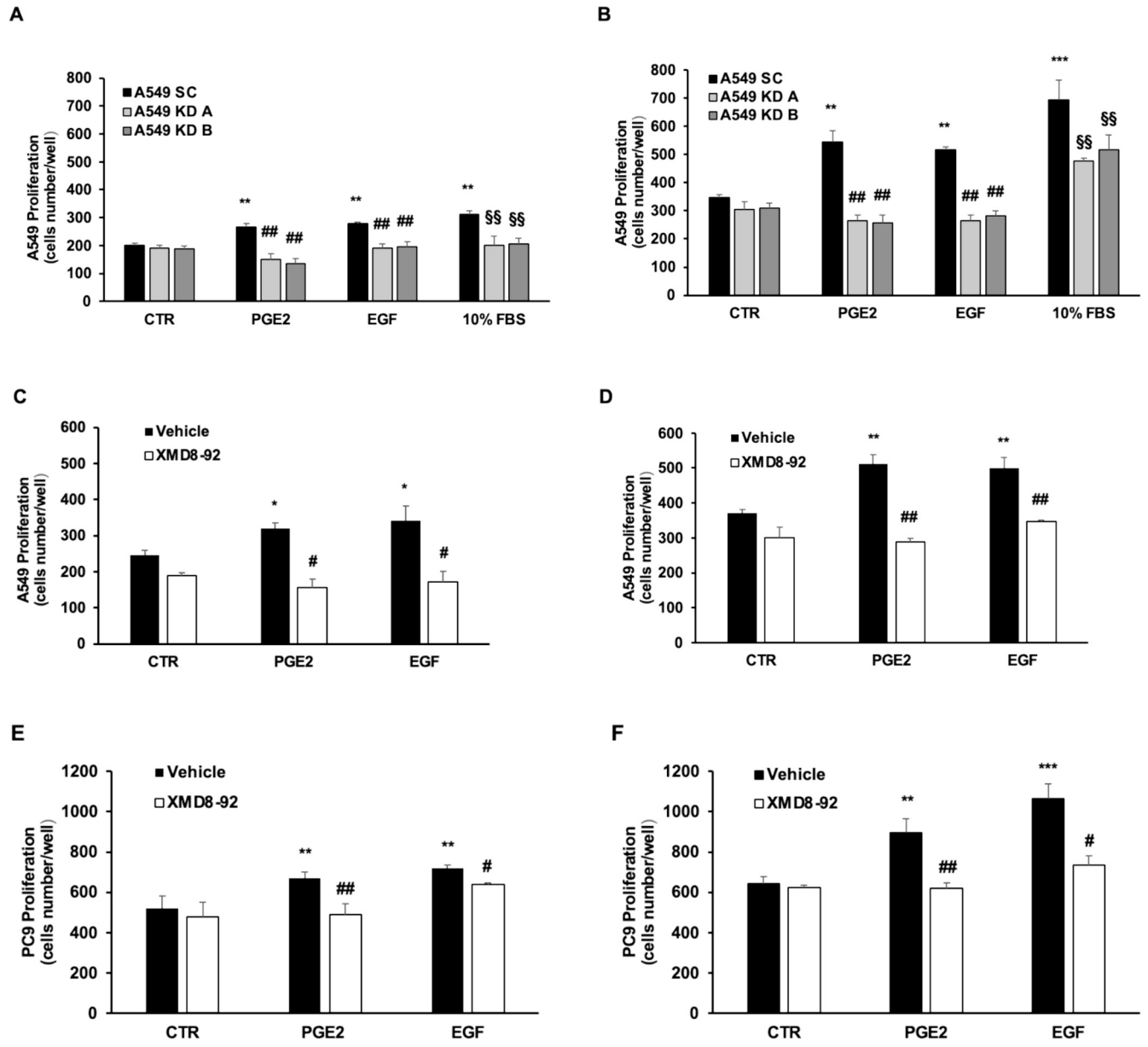

Fig. 2. PGE2 induces NSCLC proliferation and cell cycle progression through ERK5 activation. A549 (SC, ERK5KD A and B) cell proliferation after 24 (A) and 48 (B) hours of treatment with PGE2 (1 μM) or EGF (25 ng/ml) in 1 % FBS. $^{**}p < 0.01$ vs untreated cells (CTR condition) and ## $p < 0.01$ vs A549 SC treated with PGE2 or EGF; §§ $p < 0.01$ vs A549 SC treated with 10 % FBS. (C, D). Proliferation of A549 exposed to EGF (25 ng/ml) or PGE2 (1 μM) with or without XMD8-92 (5 μM, 30 min of pre-treatment) for 24 (C) and 48 (D) hours. $^{*}p < 0.05$ and $^{**}p < 0.01$ vs untreated cells (CTR condition); #$p < 0.05$ and ## $p < 0.01$ vs A549 SC treated with PGE2 or EGF alone. (E, F). Proliferation of PC9 exposed to EGF (25 ng/ml) or PGE2 (1 μM) with or without XMD8-92 (0.5 μM, 30 min of pre-treatment) for 24 (E) and 48 (F) hours. $^{**}p < 0.01$ and $^{***}p < 0.001$ vs untreated cells (CTR condition); #$p < 0.05$ and ## $p < 0.01$ vs A549 treated with PGE or EGF alone. The percentage of cells at each stage of the cell cycle was analyzed by flow cytometry after DNA staining with propidium iodide. Quantification of cells residing in S phase (G) and G_0/G_1 (H) of cell cycle for A549 SC exposed to XMD8-92 (5 μM, 30 min of pre-treatment), PGE2 (1 μM) or their combination for 24 h. $^{*}p < 0.05$ vs untreated cells (CTR condition). # $p < 0.05$ vs A549 SC treated with PGE2. (I). Quantification of cells residing in different phases of cell cycle G_0 for A549 ERK5 KD exposed to PGE2 (1 μM) for 24 h. (J). c-Myc gene expression in A549 cells (SC, KD A and B) treated with PGE2 (0.1 μM and 1 μM) for 24 h. $^{***}p < 0.001$ vs untreated cells (CTR condition). ### $p < 0.001$ vs A549 SC treated with PGE2. (K). c-Myc (57 kDa) protein expression in A549 cells (SC, KD A) treated with PGE2 and EP1 receptor agonist (0 1 μM) for 48 h. (L). Quantification of blot reported in (K). CTR condition has assigned 1. $^{*}p < 0.05$ vs CTR. β-actin (45 kDa) was used as loading control. Blots are representatives of three independent experiments. Molecular weight markers on the left of blots.

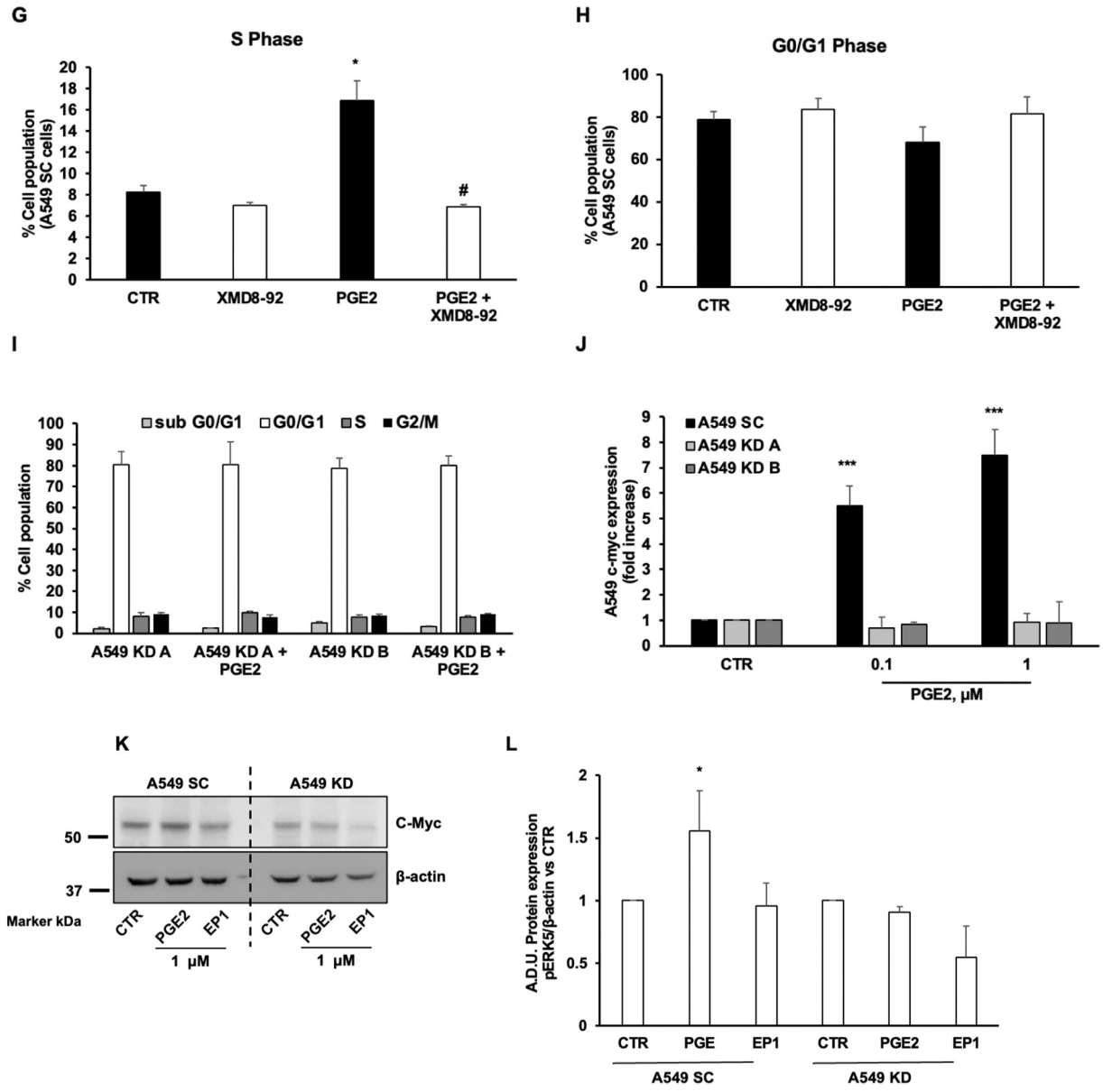

Fig. 2. (*continued*).

by its phosphorylation at MEK5-consensus residues (Thr219/Tyr 221) (Fig. 1H,I) and at the autophosphorylation site Ser496 (Supplementary Fig. 2A,B) [39]. Consistently with the above results, 15 min exposure to PGE2 and EP1 promoted the phosphorylation of p90RSK and SGK1 in A549 SC (Fig. 1H), and of SGK1 in PC9 (Fig. 1I). Interestingly, 60 min exposure to PGE2 and EP1 increased the expression of KLF2, a target of ERK5-dependent transcriptional regulation, in A549 SC, but not in A549 KD cells (Fig. 1J).

These results indicated that PGE2 promoted ERK5 signaling activation mainly via EP1 receptor in NSCLC cells.

3.2. PGE2 induces ERK5-dependent NSCLC cell proliferation and cell cycle progression

The pro-tumoral properties of PGE2 have been extensively documented in several reports describing its effect by multiple mechanisms in vitro and in vivo models [40–42]. We then assessed whether ERK5 mediates the PGE2-induced lung cancer cell growth.

At 24 and 48 h in 1 % FBS, PGE2 induced NSCLC cell proliferation (Fig. 2A and B) as previously reported [10].Time-dependent increase in the number of A549 cells cultured under PGE2 stimulation was significantly reduced upon ERK5 KD, while basal growth was not affected. This lack of effect, obtained using low FBS concentration (i.e. 1 %) serum, is at variance with a previous report in which, in high serum (10 % FBS) knockdown of ERK5 significantly reduced basal growth [35], similar to what observed in our experimental settings using 10 % FBS. As expected, ERK5KD impaired EGF-induced growth in A549 cells (Fig. 2A and B). Similar results were obtained following pharmacological inhibition of ERK5 kinase activity using XMD8-92. Indeed, XMD8-92 treatment abolished the proliferation induced by PGE2 and EGF after 24 and 48 h of treatment in both A549 (Fig. 2C and D) and PC9 cells (Fig. 2E and F).

The relevance of PGE2/ERK5 axis in the control of proliferation in A549 cells was further investigated monitoring the effects on cell cycle. Treatment with PGE2 resulted in an increase of the percentage of cells in the S phase (Fig. 2G) and in a decrease, although not statistically significant, in the proportion of cells in G0/G1 phase (Fig. 2H). In XMD8-92-treated NSCLC cells, PGE2 failed to improve cell cycle progression. In line with these observations, genetic inhibition of ERK5 determined an inability of PGE2 to promote G1 to S-phase transition in A549 cells (Fig. 2I). Finally, PGE2 caused a slight, but not significant increase, of

cells residing in G2/M phase (Supplementary Fig. 3). The induction of cell proliferation by promoting G1/S-phase transition during cell cycle progression is one of c-Myc best characterized function, a feature linked to its pro-oncogenic activity [43]. Consistently, PGE2 (at 0.1 and 1 μM) showed a significant increase of c-Myc mRNA in A549 cells which was abolished in ERK5 KD clones (Fig. 2J). Additionally, an increased expression of c-MYC was observed in A549 SC, but not in ERK5 KD cells exposed to PGE2 (Fig. 2K).

These results demonstrated that PGE2 promoted NSCLC cell proliferation and cell cycle progression at least in part by activating ERK5.

3.3. Involvement of ERK5 in cell migration and invasion in response to PGE2

To further explore the possible contribution of PGE2/ERK5 axis to the aggressive phenotype of NSCLC cells, we investigated the effects of ERK5 silencing or pharmacological inhibition of its kinase activity on the capacity of NSCLC cells to migrate under PGE2 stimulation. In wound healing assay, PGE2 promoted A549 SC migration by speeding up the scratch closure process after 18 h (Fig. 3A and B). ERK5 silencing impaired the ability of PGE2 to induce migration of A549 cells. Moreover, ERK5 inhibition with XMD8-92 was associated with a significant reduction of PC9 motility (Fig. 3C and D), further supporting a critical role of ERK5 in PGE2-induced NSCLC cell migration.

Next, we investigated the role of ERK5 in modulating the invasive phenotype of NSCLC cells exposed to PGE2, using the Boyden chamber and gelatin-coated filters. As reported in literature, we found that PGE2 exposure significantly increased the number of A549 (Fig. 3E) and PC9 (Fig. 3F) invading cells [44]. Furthermore, using selective EP receptor agonists EP1 agonist promoted A549 and PC9 invasion, while EP4 agonist showed a significant increase of PC9 motility, indicating their relevance for PGE2-mediated invasion (Fig. 3E and F). Pharmacological inhibition of ERK5 by XMD8-92 abolished NSCLC cell mobilization, demonstrating an involvement of ERK5 activation in PGE2-mediating invasion.

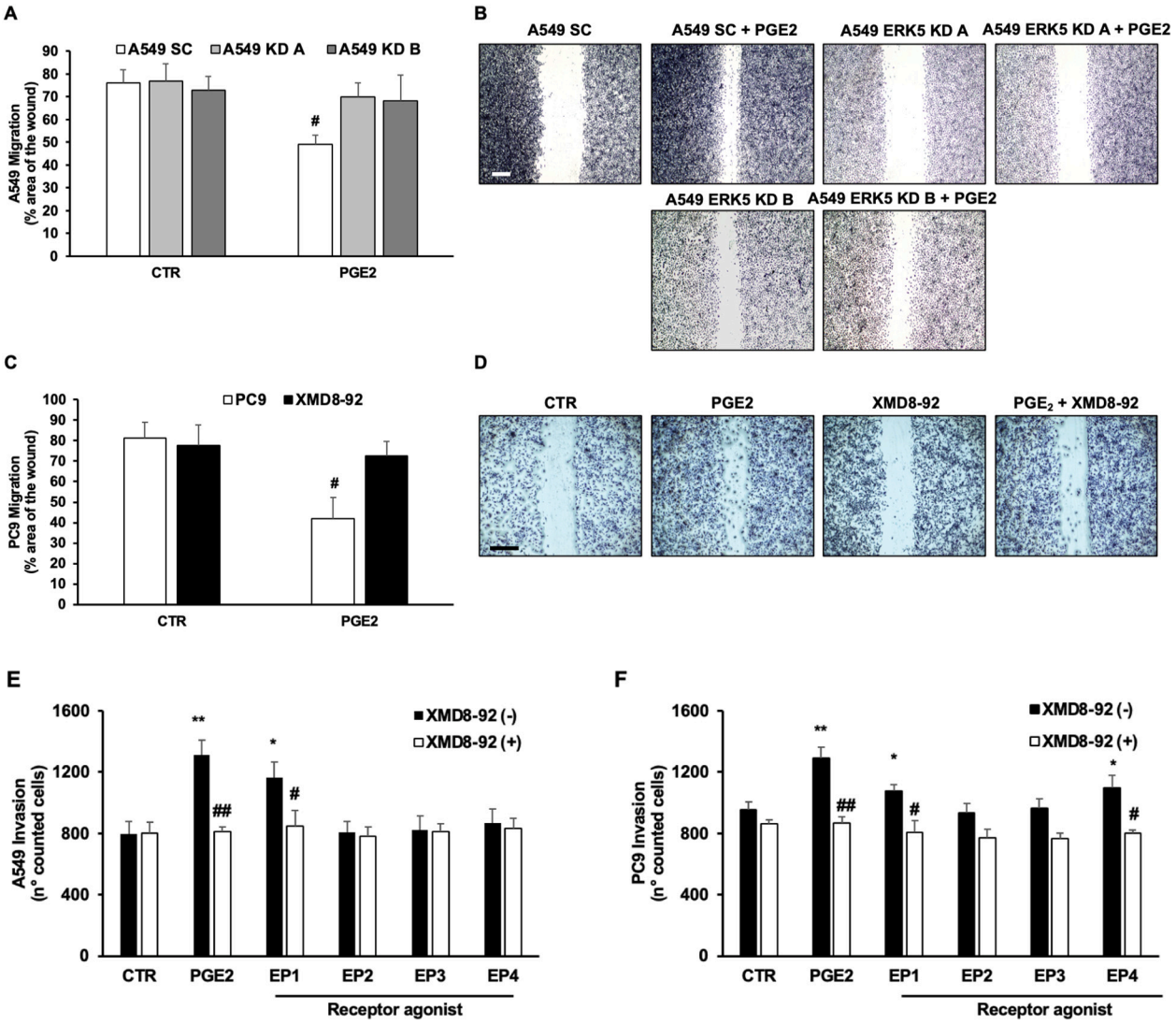

Fig. 3. PGE2 promotes NSCLC cell migration and invasion by activating EP1 and ERK5 signaling. (A, B). Scratch closure after 18 h of PGE2 treatment (1 μM) in A549 (SC, ERK5 KD A and B) cells. #$p < 0.05$ vs untreated cells (CTR condition). Scale bar, 100 μm. (C, D). PC9 cells scratch closure exposed to PGE2 (1 μM) for 18 h (1 % FBS) with or without XMD8-92 (0.5 μM, 30 min of pre-treatment). *$p < 0.05$ vs untreated cells (Ctr condition). (E). Tumor cell invasion evaluated by Boyden chamber assay in A549 SC exposed to EP receptors agonists (1 μM) for 8 h (1 % FBS) with or without XMD8-92 (5 μM, 30 min of pre-treatment). *$p < 0.05$ and **$p < 0.01$ vs untreated cells (Ctr condition); #$p < 0.05$ and ##$p < 0.01$ vs A549 treated with PGE2 or EP receptor agonist alone. (F). Invasion of PC9 cells. Cells were exposed to EP receptors agonists (1 μM) for 8 h (1 % FBS) with or without XMD8-92 (0.5 μM, 30 min of pre-treatment). *$p < 0.05$ and **$p < 0.01$ vs untreated cells (CTR condition); #$p < 0.05$ and ##$p < 0.01$ vs A549 treated with PGE2 or EP receptor agonist alone.

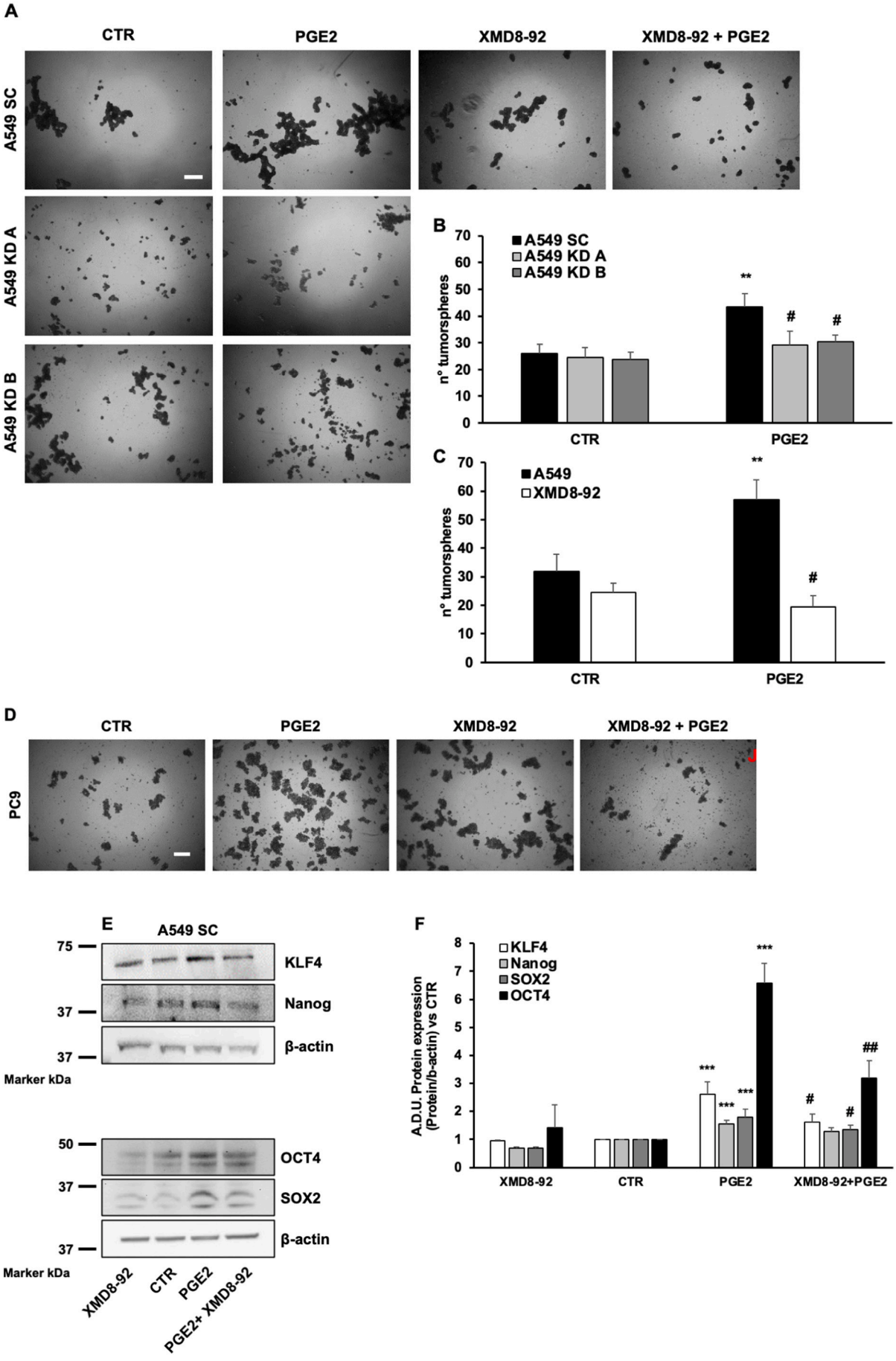
A
CTR
PGE2
XMD8-92
XMD8-92 + PGE2
A549 SC
A549 KD A
A549 KD B
B
A549 SC
A549 KD A
A549 KD B
n° tumorspheres
CTR
PGE2
C
A549
XMD8-92
n° tumorspheres
CTR
PGE2
D
CTR
PGE2
XMD8-92
XMD8-92 + PGE2
PC9
E
A549 SC
KLF4
Nanog
β-actin
Marker kDa
OCT4
SOX2
β-actin
Marker kDa
XMD8-92
CTR
PGE2
PGE2+ XMD8-92
F
KLF4
Nanog
SOX2
OCT4
A.D.U. Protein expression (Protein/b-actin) vs CTR
XMD8-92
CTR
PGE2
XMD8-92+PGE2

Fig. 4. PGE2 enhances NSCLC cells in vitro stemness and clonogenicity in ERK5-dependent manner. (A). Representative images of tumorspheres (4× magnification) showing morphology of A549 SC or ERK5 KD (A and B) spheres grown for 7 days on ultra-low attachment plate exposed to PGE2 (1 μM) or not for 7 days or A549 spheroids treated with PGE2 (1 μM), XMD8-92 (5 μM) or their combination for 7 days. Scale bar, 100 μm. (B). Quantification of A549 tumorspheres number. Ten pictures for each well were quantified. $^{**}p < 0.01$ vs A549 SC untreated cells (CTR condition); $\#p < 0.05$ vs A549 SC treated with PGE2. (C). Quantification of A549 tumorspheres treated with XMD8-92. $^{**}p < 0.01$ vs A549 SC untreated cells (CTR condition); $\#p < 0.05$ vs A549 SC treated with PGE2 alone. (D). Representative images of tumorspheres (4× magnification) showing the morphology of PC9 spheres grown for 7 days on ultra-low attachment plate treated with PGE2 (1 μM), XMD8-92 (0.5 μM) or their combination. Scale bar, 100 μm. (E). Western Blot analysis of stemness markers KLF4 (65 kDa) and Nanog (42 kDa), and SOX2 (35 kDa) and OCT4 (45 kDa) in A549 SC cells exposed to XMD8-92 (5 μM), PGE2 (1 μM) or their combination for 7 days. (F). Quantification of blots reported in E. β-actin (45 kDa) was used as loading control. Blot representatives of three independent experiments. $^{***}p < 0.01$ vs untreated cells (CTR condition); $\#p < 0.05$ and $\#\#p < 0.01$ vs A549 treated with PGE2 alone. Molecular weight markers on the left of blots. (G). Confocal β-catenin analysis in A549 cells treated with PGE2 for 4 h. Representative images of three experiments at 63× magnification are shown. Scale bar: 20 μm. (H). Clone formation in A549 SC, ERK5 KD A or B exposed to PGE2 (1 μM) for 10 days. Scale bar, 100 μm. Quantification of clone diameter (I) and number (J) of A549 cell. $^{*}p < 0.05$ and $^{**}p < 0.01$ vs untreated A549 SC. $\#\#p < 0.01$ vs A549 SC treated with PGE2.

3.4. PGE2 promotes lung cancer stem-like cell phenotypes and clonogenic properties through ERK5

Three-dimensional sphere models are widely used to promote the growth of tumor cell populations with stem-like properties in vitro. NSCLC cells were cultured in low attachment conditions and exposed to PGE2. Under these experimental settings, compared with untreated cells, PGE2 increased the ability of A549 and PC9 to form tumorspheres, evaluated by number of spheres and their size (an index of CSC expansion) (Fig. 4A–C for A549 and Fig. 4D for PC9).

The contribution of ERK5 in the regulation of the stemness phenotype induced by PGE2 was established in NSCLC cells co-treated with XMD8-92, in which a significant reduction in spheres formation was found (Fig. 4A–C for A549 and Fig. 4D for PC9). Similarly, PGE2 was unable to induce spheres formation in A549 ERK5KD cells (Fig. 4A–C). We also observed a significant increase expression of KLF4, OCT4, SOX2, and Nanog in PGE2-treated A549 (Fig. 4E–F). XMD8-92 exposure causes a significant reduction of KLF4 OCT4 and SOX2 expression (Fig. 4E-F). The Wnt/β-catenin signaling plays a pivotal role in stemness and cell plasticity [45]. Interestingly, PGE2 promoted β-catenin intracellular redistribution from cell membrane to perinuclear area in A549 SC, while its activity was reduced in A549 KD cells (Fig. 4G), indicating that β-catenin mobilization induced by PGE2 is dependent on ERK5 activation [46]. However, whether this effect is linked to PGE2-induced stemness features remains to be addressed.

Next, we focused on clonal expansion capacity of A549 cells, and found maximum clonal induction under PGE2 stimulation in A549 cells (Fig. 4H–J). In contrast, A549 ERK5KD cells showed a lower clonogenic capacity even when treated with PGE2 (Fig. 4H–J).

Taken together these findings indicate that PGE2 mediates lung cancer cell stemness and clonogenic capability through activation of ERK5.

4. Discussion

PGE2, a key inflammatory mediator and the principle metabolic product of the COX enzyme, has been established as playing a major role in cancer, with cancer-promoting PGE2-mediated inflammation an enabling characteristic underlying many, if not all, the hallmarks of cancer. Both PGE2 and ERK5 are known to be involved in several cellular processes, including cell proliferation, differentiation, survival, migration, mesenchymal transition, stemness, angiogenesis, and suppression of host immunity both in normal and in neoplastic cells [5,15,17,31,41,47–50].

In this study, we demonstrated that PGE2 promotes ERK5 activation through EP1 receptor and that this activation is central for prostanoid-mediated functions, such as proliferation, invasion, and induction of a stem-like phenotype in a preclinical model of NSCLC cells, namely A549 and PC9 cells.

In lung cancer, activation of ERK5 promotes cell proliferation, while inhibition of its kinase activity or silencing of its expression correlates with inhibition of proliferation in several lung adenocarcinoma models, both in vitro and in vivo studies [35,51]. At the clinical level, overexpression of MEK5/ERK5 is linked to a poor prognosis for lung cancer patients [35,52,53]. High combined expression levels of MEK5 and ERK5 are significantly associated with poor overall survival of patients with lung adenocarcinoma [52], and the levels of ERK5 and phosphorylated ERK5 are higher in lung cancer tissues than in normal lung tissues and much higher in high-grade lung cancer tissues than in low-grade lung cancer tissues [53], clearly indicating that ERK5 activation correlates with lung cancer malignancy.

In this study, we show that PGE2, whose activity in lung adenocarcinoma cell proliferation was previously demonstrated by us, as well as by other laboratories [10,54–56], promotes ERK5 activation and the growth of A549 and PC9 cells, and that pharmacological inhibition of ERK5 through the inhibitor XMD8-92, as well as ERK5 knockdown reduces their growth. Of note, in high proliferative condition (10 % FBS) an increased proliferation arose in untreated ERK5 SC cells, which is not reported in A549 KD. This modulation is not observable in 1 % serum condition (our control condition), revealing a serum-dependency effect that arose only in high proliferative conditions, according with Sánchez-Fdez reported analysis [35].

Both the antibody to total ERK5 to highlight the presence of un upshifted band upon ERK5 phosphorylation and the antiphospho-ERK5 antibody against p-ERK5$^{Thr218/Y220}$ (that recognizes MEK5-dependent phosphorylation sites Thr219/Y221) and p-ERK5^{Ser496} consistently demonstrate the functional correlation between exposure of A549 and PC9 to PGE2 and activation of ERK5. On the other hand, the use of two silencers for ERK5 expression and the pharmacological inhibitor XMD8-92 further confirmed the mechanistic involvement of ERK5 in the pro-tumorigenic activities of PGE2 in the two cellular models under study. Additionally, despite XMD8-92 has been reported to be a dual ERK5/BRD inhibitor, although largely used to study ERK5 [13,57], genetic know down of ERK5 was able to recapitulate all the effects determined by XMD8-92 thus demonstrating the key role of ERK5 activation in all the PGE2-dependent biological process analyzed in the study.

XMD8-92 was used to block ERK5 activity rather than to prevent its phosphorylation by MEK5 at a specific residue, as well as its KD. Indeed, the aim of this manuscript was to demonstrate the existence of a functional link between PGE2 and ERK5, i.e. to demonstrate the mechanistic role of ERK5 in the pro-tumor activity of this inflammation mediator. We found that PGE2 induces ERK5 phosphorylation at both MEK5-consensus residues (i.e. Thr219/Tyr221) and Ser496. The fact that ERK5 is phosphorylated at Ser496 upon PGE2 administration is an intriguing finding because this site has been reported to be both autophosphorylated and a substrate for p90RSK [39,58], the latter found to be phosphorylated, in turn, following PGE2 administration to NSCLC cells. We are aware, however, that we did not provide demonstration that these are the only phosphorylating events involved in PGE2-dependent pro-tumorigenic activities involving ERK5, so that this aspect deserves further investigation.

A variety of downstream cytosolic or nuclear substrates, such as the

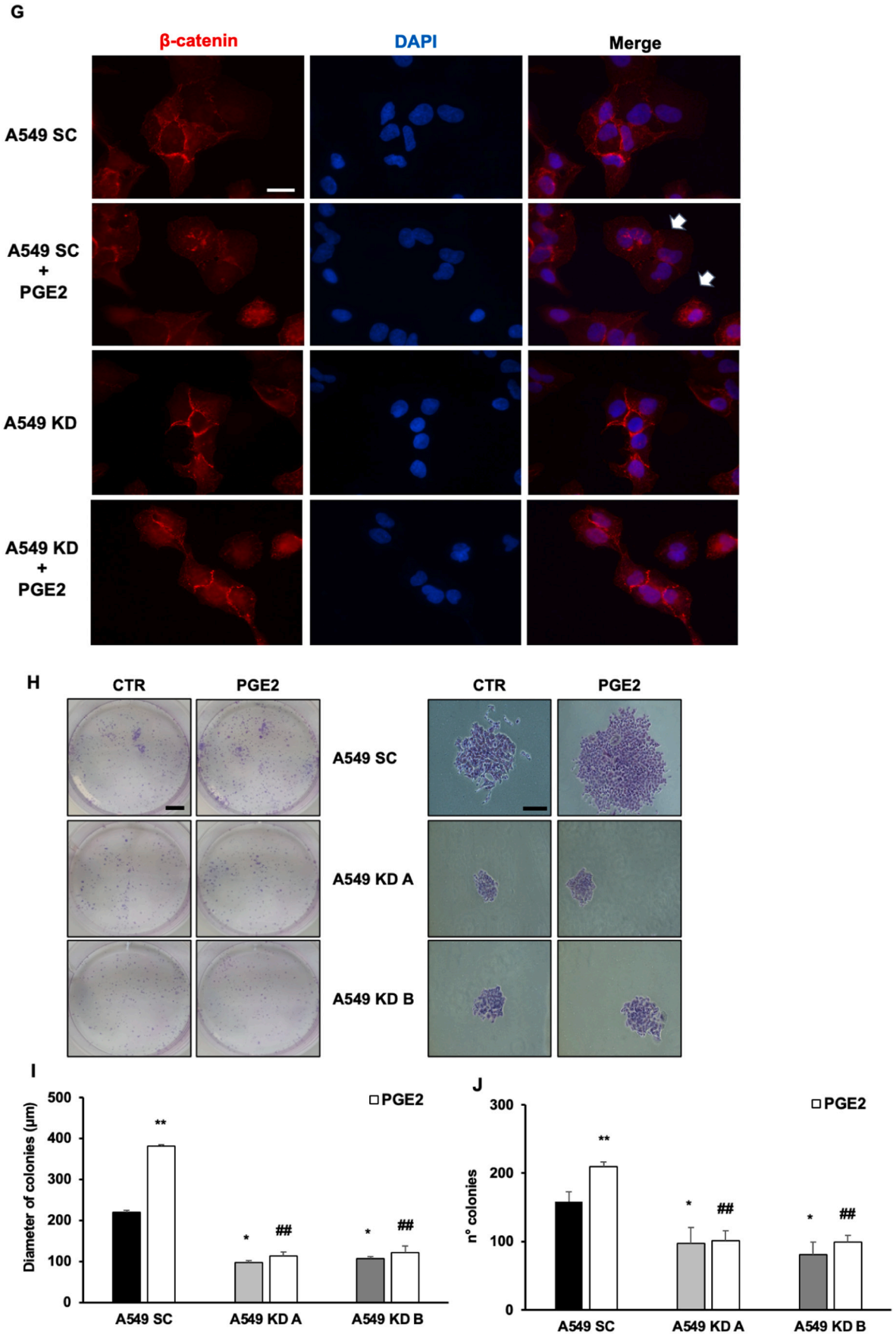

Fig. 4. (*continued*).

protein kinases p90RSK and SGK are phosphorylated by the MAPKs, including ERK5, to elicit a range of cellular responses [58,59]. In agreement, in A549 and PC9, exposure to PGE2 and EP1 also promoted the phosphorylation of p90RSK and SGK1. Additionally, ERK5 was proposed to control G1-S cell cycle progression by the regulation of SGK1 [60]. Through cell cycle analysis, we have shown that inhibition of ERK5 activity affects the S and G0/G1 phases of cell growth, in line with our and previous evidence [61]. Indeed, both A549 and PC9 exposed to PGE2 show an increase in S-phase and a concomitant reduction in the proportion of cells in G_0/G_1 phase, which are reverted either by the presence of XMD8-92 or by ERK5 depletion through its silencing. ERK5 expression and activity is related to the transcription of a variety of effectors, including KLF2 and the proto-oncogene c-Myc expression and c-Myc protein stabilization in several cancer cell models [57,62]. In A549 lung cancer cells, PGE2 significantly promotes KLF2 and c-Myc expression, which are suppressed by depletion of ERK5, indicating that this effect is mediated by the expression of the kinase. Dowregulation of c-Myc mRNA below levels measured under control conditions indicate that this protooncogene is strongly associated with the expression and activity of ERK5 and reinforce the findings on the antiproliferative effect of ERK5 depletion or pharmacological inhibition on lung adenocarcinoma cells exposed to both PGE2 and high serum. Furthermore, the low amount of c-MYC in ERK5 KD cells exposed to PGE2 corroborated our data according with published evidence [10]. Of note, compensatory mechanisms involved into the regulation of c-MYC exist, and other members of ERK family could play a key role in this game, replacing the absence of ERK5 [63].

Elevated ERK5 expression in lung cancer was linked to the acquisition of increased metastatic and invasive potential [53]. Our results also show that ERK5 activation is required for the invasion of A549 and PC9 cells, studied by means of the scratch and the Boyden chamber assays. In both assays, exposure of the cells to PGE2 promotes their invasion, which is abolished by co-treatment of the cells with ERK5 inhibitor or gene silencing. ERK5 is reported in the literature to activate the epithelial-mesenchymal transition in many tumor models, and only in few models there are indications suggesting an active role of ERK5 in the cytoskeleton rearrangements, prodromal to cell motility and invasion [64–68]. We and others have shown that PGE2 instead can promote both the epithelial-mesenchymal transition process in lung adenocarcinoma cells and the rearrangement of their cytoskeleton [40,69]. Further studies will be necessary to assess whether PGE2-induced ERK5 activation is mainly involved in the control of epithelial-mesenchymal transition and/or cytoskeleton rearrangement in the A549 and PC9 cell invasion.

There are no indications in the literature on the role of ERK5 in the stem phenotype of lung cancer cells, and overall, few studies indicate a contribute of MEK5/ERK5 signaling in cancer stemness [50,70–72]. Recently Fukasawa and colleagues demonstrated that MEK5-ERK5-STAT3 pathway plays an essential role in maintaining glioma stem cell stemness and tumorigenicity, and that pharmacologic inhibition of ERK5 significantly inhibited glioma stem cell self-renewal and growth [73]. In this study we show that PGE2 promotes a stem-like phenotype in A549 and PC9 cells and that this process is mediated, at least in part, by ERK5 activation. In fact, we show that both A549 and PC9 cells when exposed to PGE2 acquire the ability to form tumorspheres in a low attachment culture system and express markers of stemness such as Nanog, OCT4, SOX2, and KLF4. Co-treatment with XMD8-92 or silencing of ERK5 significantly reduces both tumorsphere formation capacity and marker expression. In the clonogenic assay, a model of self-renewal for tumor cells, ERK5 silencing markedly reduces both clone diameters and numbers, indicating that PGE2 mediates A549 lung cancer cell stemness and clonogenic capability through activation of ERK5.

PGE2 mediates its biological functions through the activation of four G-protein-coupled receptors, EP1–4. Several signals are downstream to PGE2/EPs axis, unveil a redundancy in PGE2-mediated tumorigenic properties in cancer. We already demonstrated in A549 that PGE2 mainly through EP3 receptor promotes EGFR internalization and cancer cell proliferation [10,74]. In this, our results show that the activation of ERK5 by PGE2 in A549 and PC9 is mainly mediated by EP1 receptor. Indeed, by using agonists for the four EPs receptors, we show that only the EP1 agonist can promote phosphorylation of ERK5, and that in the cell invasion model it promotes invasion of A549 and PC9 cells and that this effect is reduced by treatment with XMD8-92. The molecular mechanism involved in PGE2/EP1 activation of ERK5 was not investigated, but several hypotheses can be made. EP1 receptors couple to Gαq protein and mediate signaling events by activation of PLC. This results in the elevation of cytoplasmic signaling intermediates including IP3 and DAG, an increase in intracellular Ca2+, leading to the activation of PKC [9]. Furthermore, EP1 activation of PKC was linked to src and EGFR transactivation, and ERK5 is known to be an important component of the pathway of various cellular signals activated by EGFR [9,75,76]. In our cellular models, whether EP1-induced PKC activation is directly involved in the phosphorylation of ERK5, or whether this activation is mediated by the transactivation of EGFR by PGE2 has not been investigated and will require further study.

5. Conclusions

In conclusion, the above findings demonstrate that ERK5 activation is involved in PGE2- mediated proliferation, invasion and gain of a stem-like phenotype in human lung adenocarcinoma cells. Mechanistically, activation of ERK5 by PGE2 is mainly mediated by EP1 receptor. Further analysis is needed to dissect PGE2/EP1 signaling leading to ERK5 activation, and the functional role of different phosphorylating events within the ERK5 protein in mediating PGE2's pro-tumorigenic effects. Targeting this axis for inhibition holds promise as a potential avenue for the development of novel therapeutic agents aimed at control the advancement of NSCLC.

Funding

The research leading to these results has received funding from Associazione Italiana per la Ricerca sul Cancro (AIRC) and Fondazione CR Firenze under IG 2018–ID 21349 project (P.I. Rovida Elisabetta), European Union-Next Generation EU-National Recovery and Resilience Plan, Mission 4 Component 2-Investment1.5-THE-Tuscany Health Ecosystem-ECS00000017-CUP B83C22003920001 to ER.

CRediT authorship contribution statement

Arianna Filippelli: Writing – review & editing, Writing – original draft, Validation, Methodology, Investigation, Formal analysis, Data curation. **Valerio Ciccone:** Writing – review & editing, Writing – original draft, Validation, Methodology, Investigation, Formal analysis, Data curation. **Cinzia Del Gaudio:** Methodology, Investigation, Formal analysis, Data curation. **Vittoria Simonis:** Validation, Methodology, Investigation, Data curation. **Maria Frosini:** Writing – original draft, Validation, Methodology, Investigation, Formal analysis, Data curation. **Ignazia Tusa:** Writing – review & editing, Validation, Methodology, Investigation, Formal analysis, Data curation. **Alessio Menconi:** Methodology, Investigation. **Elisabetta Rovida:** Writing – review & editing, Supervision, Resources, Project administration, Funding acquisition, Data curation. **Sandra Donnini:** Writing – review & editing, Writing – original draft, Visualization, Validation, Project administration, Methodology, Data curation, Conceptualization.

Declaration of competing interest

The authors declare that they have no known competing financial interests or personal relationships that could have appeared to influence the work reported in this paper.

Data availability

Data will be made available on request.

Acknowledgments

Fondazione Umberto Veronesi, Milan (Italy) for Valerio Ciccone Post-doctoral Fellowship (2023).

Appendix A. Supplementary data

Supplementary data to this article can be found online at https://doi.org/10.1016/j.bbamcr.2024.119810.

References

[1] C.S. Dela Cruz, L.T. Tanoue, R.A. Matthay, Lung cancer: epidemiology, etiology, and prevention, Clin. Chest Med. 32 (4) (2011 Dec), https://doi.org/10.1016/j.ccm.2011.09.001.
[2] F.R. Greten, S.I. Grivennikov, Inflammation and cancer: triggers, mechanisms and consequences, Immunity 51 (1) (2019 Jul 16) 27–41.
[3] S.I. Grivennikov, F.R. Greten, M. Karin, Immunity, inflammation, and cancer, Cell 140 (6) (2010 Mar 19) 883–899.
[4] Á. Jara-Gutiérrez, V. Baladrón, The role of prostaglandins in different types of cancer, Cells 10 (6) (2021 Jun 13) 1487.
[5] F. Finetti, E. Terzuoli, E. Bocci, I. Coletta, L. Polenzani, G. Mangano, et al., Pharmacological inhibition of microsomal prostaglandin E synthase-1 suppresses epidermal growth factor receptor-mediated tumor growth and angiogenesis, PloS One 7 (7) (2012) e40576.
[6] D. Wang, R.N. DuBois, Role of prostanoids in gastrointestinal cancer, J. Clin. Invest. 128 (7) (2018 Jul 2) 2732–2742.
[7] R. Mizuno, K. Kawada, Y. Sakai, Prostaglandin E2/EP signaling in the tumor microenvironment of colorectal cancer, Int. J. Mol. Sci. 20 (24) (2019 Dec 11) 6254.
[8] H. Yokouchi, K. Kanazawa, Revisiting the role of COX-2 inhibitor for non-small cell lung cancer, Transl. Lung Cancer Res. 4 (5) (2015 Oct) 660–664.
[9] G. O'Callaghan, A. Houston, Prostaglandin E2 and the EP receptors in malignancy: possible therapeutic targets? Br. J. Pharmacol. 172 (22) (2015 Nov) 5239–5250.
[10] L. Bazzani, S. Donnini, F. Finetti, G. Christofori, M. Ziche, PGE2/EP3/SRC signaling induces EGFR nuclear translocation and growth through EGFR ligands release in lung adenocarcinoma cells, Oncotarget 8 (19) (2017 May 9) 31270–31287.
[11] G. Digiacomo, M. Ziche, P. Dello Sbarba, S. Donnini, E. Rovida, Prostaglandin E2 transactivates the colony-stimulating factor-1 receptor and synergizes with colony-stimulating factor-1 in the induction of macrophage migration via the mitogen-activated protein kinase ERK1/2, FASEB J. 29 (6) (2015 Jun) 2545–2554.
[12] D.P. Cherukuri, X.B. Chen, A.C. Goulet, R.N. Young, Y. Han, R.L. Heimark, J. W. Regan, E. Meuillet, M.A. Nelson, The EP4 receptor antagonist, L-161,982, blocks prostaglandin E2-induced signal transduction and cell proliferation in HCA-7 colon cancer cells, Exp. Cell Res. 313 (14) (2007 Aug 15) 2969–2979, https://doi.org/10.1016/j.yexcr.2007.06.004.
[13] A. Tubita, Z. Lombardi, I. Tusa, P. Dello Sbarba, E. Rovida, Beyond kinase activity: ERK5 nucleo-cytoplasmic shuttling as a novel target for anticancer therapy, Int. J. Mol. Sci. 21 (3) (2020 Jan 31) 938.
[14] B.A. Drew, M.E. Burow, B.S. Beckman, MEK5/ERK5 pathway: the first fifteen years, Biochim. Biophys. Acta 1825 (1) (2012 Jan) 37–48.
[15] N. Gomez, T. Erazo, J.M. Lizcano, ERK5 and cell proliferation: nuclear localization is what matters, Front. Cell Dev. Biol. 4 (2016) 105.
[16] Y.J. Guo, W.W. Pan, S.B. Liu, Z.F. Shen, Y. Xu, L.L. Hu, ERK/MAPK signalling pathway and tumorigenesis (review), Exp. Ther. Med. 19 (3) (2020 Mar 1) 1997–2007.
[17] B. Stecca, E. Rovida, Impact of ERK5 on the hallmarks of cancer, Int. J. Mol. Sci. 20 (6) (2019 Mar 21) 1426.
[18] Z. Lombardi, L. Gardini, A.V. Kashchuk, A. Menconi, M. Lulli, I. Tusa, et al., Importin subunit beta-1 mediates ERK5 nuclear translocation, and its inhibition synergizes with ERK5 kinase inhibitors in reducing cancer cell proliferation, Mol. Oncol. (2024 Jul 4), https://doi.org/10.1002/1878-0261.13674.
[19] L. Benito-Jardón, M. Díaz-Martínez, N. Arellano-Sánchez, P. Vaquero-Morales, A. Esparís-Ogando, J. Teixidó, Resistance to MAPK inhibitors in melanoma involves activation of the IGF1R–MEK5–Erk5 pathway, Cancer Res. 79 (9) (2019 May 1) 2244–2256.
[20] A. Tubita, I. Tusa, E. Rovida, Playing the whack-a-mole game: ERK5 activation emerges among the resistance mechanisms to RAF-MEK1/2-ERK1/2- targeted therapy, Front. Cell Dev. Biol. 9 (2021) 647311.
[21] I. Tusa, A. Menconi, A. Tubita, E. Rovida, Pathophysiological impact of the MEK5/ERK5 pathway in oxidative stress, Cells 12 (8) (2023 Apr 13) 1154.
[22] E. Giurisato, Q. Xu, S. Lonardi, B. Telfer, I. Russo, A. Pearson, et al., Myeloid ERK5 deficiency suppresses tumor growth by blocking protumor macrophage polarization via STAT3 inhibition, Proc. Natl. Acad. Sci. U. S. A. 115 (12) (2018 Mar 20) E2801–E2810.
[23] K.G. Finegan, D. Perez-Madrigal, J.R. Hitchin, C.C. Davies, A.M. Jordan, C. Tournier, ERK5 is a critical mediator of inflammation-driven cancer, Cancer Res. 75 (4) (2015 Feb 15) 742–753.
[24] Q. Yang, X. Deng, B. Lu, M. Cameron, C. Fearns, M.P. Patricelli, et al., Pharmacological inhibition of BMK1 suppresses tumor growth through promyelocytic leukemia protein, Cancer Cell 18 (3) (2010 Sep 14) 258–267.
[25] V. Ciccone, M. Zazzetta, L. Morbidelli, Comparison of the effect of two hyaluronic acid preparations on fibroblast and endothelial cell functions related to angiogenesis, Cells 8 (12) (2019 Nov 21) 1479.
[26] E. Terzuoli, G. Nannelli, M. Frosini, A. Giachetti, M. Ziche, S. Donnini, Inhibition of cell cycle progression by the hydroxytyrosol-cetuximab combination yields enhanced chemotherapeutic efficacy in colon cancer cells, Oncotarget 8 (47) (2017 Oct 10) 83207–83224.
[27] A. Filippelli, V. Ciccone, S. Loppi, L. Morbidelli, Characterization of the safety profile of sweet chestnut wood distillate employed in agriculture, Safety 7 (4) (2021 Dec) 79.
[28] V. Barbetti, I. Tusa, M.G. Cipolleschi, E. Rovida, P. Dello Sbarba, AML1/ETO sensitizes via TRAIL acute myeloid leukemia cells to the pro-apoptotic effects of hypoxia, Cell Death Dis. 4 (3) (2013 Mar 14) e536, https://doi.org/10.1038/cddis.2013.49.
[29] V. Ciccone, A. Filippelli, C. Bacchella, E. Monzani, L. Morbidelli, The nitric oxide donor [Zn(PipNONO)cl] exhibits antitumor activity through inhibition of epithelial and endothelial mesenchymal transitions, Cancers 14 (17) (2022 Jan) 4240.
[30] V. Ciccone, A. Filippelli, A. Angeli, C.T. Supuran, L. Morbidelli, Pharmacological inhibition of CA-IX impairs tumor cell proliferation, migration and invasiveness, Int. J. Mol. Sci. 21 (8) (2020 Apr 23) 2983.
[31] E. Terzuoli, F. Finetti, F. Costanza, A. Giachetti, M. Ziche, S. Donnini, Linking of mPGES-1 and iNOS activates stem-like phenotype in EGFR-driven epithelial tumor cells, Nitric Oxide 1 (66) (2017 Jun) 17–29.
[32] V. Ciccone, V. Simonis, C. Del Gaudio, C. Cucini, M. Ziche, L. Morbidelli, et al., ALDH1A1 confers resistance to RAF/MEK inhibitors in melanoma cells by maintaining stemness phenotype and activating PI3K/AKT signaling, Biochem. Pharmacol. 224 (2024 Jun) 116252.
[33] V. Ciccone, M. Monti, G. Antonini, L. Mattoli, M. Burico, F. Marini, et al., Efficacy of AdipoDren® in reducing interleukin-1-induced lymphatic endothelial hyperpermeability, J. Vasc. Res. 53 (5–6) (2016) 255–268.
[34] V. Ciccone, E. Piragine, E. Gorica, V. Citi, L. Testai, E. Pagnotta, et al., Anti-inflammatory effect of the natural H2S-donor erucin in vascular endothelium, Int. J. Mol. Sci. 23 (24) (2022 Jan) 15593.
[35] A. Sánchez-Fdez, M.F. Re-Louhau, P. Rodríguez-Núñez, D. Ludeña, S. Matilla-Almazán, A. Pandiella, et al., Clinical, genetic and pharmacological data support targeting the MEK5/ERK5 module in lung cancer, npj Precis Onc. 5 (1) (2021 Aug 17) 1–13.
[36] I. Seidita, I. Tusa, M. Prisinzano, A. Menconi, F. Cencetti, S. Vannuccini, et al., Sphingosine 1-phosphate elicits a ROS-mediated proinflammatory response in human endometrial stromal cells via ERK5 activation, FASEB J. 37 (8) (2023) e23061.
[37] Y. Kato, R.I. Tapping, S. Huang, M.H. Watson, R.J. Ulevitch, J.D. Lee, Bmk1/Erk5 is required for cell proliferation induced by epidermal growth factor, Nature 395 (6703) (1998 Oct 15) 713–716.
[38] J.K. Thompson, A. Shukla, A.L. Leggett, P.B. Munson, J.M. Miller, M. B. MacPherson, et al., Extracellular signal regulated kinase 5 and inflammasome in progression of mesothelioma, Oncotarget 9 (1) (2017 Dec 6) 293–305.
[39] N. Mody, D.G. Campbell, N. Morrice, M. Peggie, P. Cohen, An analysis of the phospho- rylation and activation of extracellular-signal-regulated protein kinase 5 (ERK5) by mitogen-activated protein kinase kinase 5 (MKK5) in vitro, Biochem. J. 372 (Pt 2) (2003 Jun 1) 567–575.
[40] S. Donnini, F. Finetti, R. Solito, E. Terzuoli, A. Sacchetti, L. Morbidelli, et al., EP2 prostanoid receptor promotes squamous cell carcinoma growth through epidermal growth factor receptor transactivation and iNOS and ERK1/2 pathways, FASEB J. 21 (10) (2007 Aug) 2418–2430.
[41] F. Finetti, E. Terzuoli, A. Giachetti, R. Santi, D. Villari, H. Hanaka, et al., mPGES-1 in prostate cancer controls stemness and amplifies epidermal growth factor receptor-driven oncogenicity, Endocr. Relat. Cancer 22 (4) (2015 Aug) 665–678.
[42] K. Krysan, R. Kusko, T. Grogan, J. O'Hearn, K.L. Reckamp, T.C. Walser, et al., PGE2-driven expression of c-Myc and OncomiR-17-92 contributes to apoptosis resistance in NSCLC, Mol. Cancer Res. 12 (5) (2014 May 1) 765–774.
[43] L. García-Gutiérrez, G. Bretones, E. Molina, I. Arechaga, C. Symonds, J.C. Acosta, et al., Myc stimulates cell cycle progression through the activation of Cdk1 and phosphorylation of p27, Sci. Rep. 9 (1) (2019 Dec 10) 18693.
[44] J.I. Kim, V. Lakshmikanthan, N. Frilot, Y. Daaka, Prostaglandin E2 promotes lung cancer cell migration via EP4-betaArrestin1-c-Src signalsome, Mol. Cancer Res. 8 (4) (2010 Apr) 569–577.
[45] R. Fodde, T. Brabletz, Wnt/beta-catenin signaling in cancer stemness and malignant behavior, Curr. Opin. Cell Biol. 19 (2) (2007 Apr) 150–158.
[46] K. Pan, W. Lee, C. Chou, Y. Yang, Y. Chang, M. Chien, et al., Direct interaction of β-catenin with nuclear ESM1 supports stemness of metastatic prostate cancer, EMBO J. 40 (4) (2021 Feb 15) e105450.
[47] S. Zelenay, A.G. van der Veen, J.P. Böttcher, K.J. Snelgrove, N. Rogers, S.E. Acton, et al., Cyclooxygenase-dependent tumor growth through evasion of immunity, Cell 162 (6) (2015 Sep 10) 1257–1270.
[48] A. Tubita, Z. Lombardi, I. Tusa, A. Lazzeretti, G. Sgrignani, D. Papini, et al., Inhibition of ERK5 elicits cellular senescence in melanoma via the cyclin-dependent kinase inhibitor p21, Cancer Res. 82 (3) (2022 Feb 1) 447–457.

[49] A. Gentilini, G. Lori, A. Caligiuri, C. Raggi, G. Di Maira, M. Pastore, et al., Extracellular signal-regulated kinase 5 regulates the malignant phenotype of cholangiocarcinoma cells, Hepatology 74 (4) (2021) 2007–2020.
[50] I. Tusa, G. Cheloni, M. Poteti, A. Gozzini, N.H. DeSouza, Y. Shan, et al., Targeting the extracellular signal-regulated kinase 5 pathway to suppress human chronic myeloid leukemia stem cells, Stem Cell Rep. 11 (4) (2018 Oct 1) 929–943.
[51] S. Cristea, G.L. Coles, D. Hornburg, M. Gershkovitz, J. Arand, S. Cao, et al., The MEK5-ERK5 kinase axis controls lipid metabolism in small-cell lung cancer, Cancer Res. 80 (6) (2020 Mar 15) 1293–1303.
[52] A. Sánchez-Fdez, M.J. Ortiz-Ruiz, M.F. Re-Louhau, I. Ramos, Ó. Blanco-Múñez, D. Ludeña, et al., MEK5 promotes lung adenocarcinoma, Eur. Respir. J. 53 (2) (2019 Feb) 1801327.
[53] W. Jiang, F. Cai, H. Xu, Y. Lu, J. Chen, J. Liu, et al., Extracellular signal regulated kinase 5 promotes cell migration, invasion and lung metastasis in a FAK-dependent manner, Protein Cell 11 (11) (2020 Nov 1) 825–845.
[54] E. Terzuoli, F. Costanza, V. Ciccone, M. Ziche, L. Morbidelli, S. Donnini, mPGES-1 as a new target to overcome acquired resistance to gefitinib in non-small cell lung cancer cell lines, Prostaglandins Other Lipid Mediat. 143 (2019 Aug) 106344.
[55] M.J. Saul, I. Baumann, A. Bruno, A.C. Emmerich, J. Wellstein, S.M. Ottinger, et al., miR-574-5p as RNA decoy for CUGBP1 stimulates human lung tumor growth by mPGES-1 induction, FASEB J. 33 (6) (2019 Jun) 6933–6947, https://doi.org/10.1096/fj.201802547R.
[56] D. Ruan, S.P. So, Prostaglandin E2 produced by inducible COX-2 and mPGES-1 promoting cancer cell proliferation in vitro and in vivo, Life Sci. 116 (1) (2014 Oct 22) 43–50, https://doi.org/10.1016/j.lfs.2014.07.042.
[57] C. Kang, J.S. Kim, C.Y. Kim, E.Y. Kim, H.M. Chung, The pharmacological inhibition of ERK5 enhances apoptosis in acute myeloid leukemia cells, Int J Stem Cells. 11 (2) (2018 Nov 30) 227–234.
[58] H.T. Vu, S. Kotla, K.A. Ko, Y. Fujii, Y. Tao, J. Medina, et al., Ionizing radiation induces endothelial inflammation and apoptosis via p90RSK-mediated ERK5 S496 phosphorylation, Front. Cardiovasc. Med. 5 (2018) 23.
[59] G.N. Nithianandarajah-Jones, B. Wilm, C.E.P. Goldring, J. Müller, M.J. Cross, ERK5: structure, regulation and function, Cell. Signal. 24 (11) (2012 Nov) 2187–2196.
[60] M. Hayashi, R.I. Tapping, T.H. Chao, J.F. Lo, C.C. King, Y. Yang, et al., BMK1 mediates growth factor-induced cell proliferation through direct cellular activation of serum and glucocorticoid-inducible kinase, J. Biol. Chem. 276 (12) (2001 Mar 23) 8631–8634.
[61] I. Tusa, S. Gagliardi, A. Tubita, S. Pandolfi, C. Urso, L. Borgognoni, et al., ERK5 is activated by oncogenic BRAF and promotes melanoma growth, Oncogene 37 (19) (2018 May) 2601–2614.
[62] R.F. Koncar, B.R. Dey, A.C.J. Stanton, N. Agrawal, M.L. Wassell, L.H. McCarl, et al., Identification of novel RAS signaling therapeutic vulnerabilities in diffuse intrinsic pontine gliomas, Cancer Res. 79 (16) (2019 Aug 15) 4026–4041.
[63] S.J. Cook, P.A. Lochhead, ERK5 signalling and resistance to ERK1/2 pathway therapeutics: the path less travelled? Front. Cell Dev. Biol. 10 (2022) 839997.
[64] V.T. Hoang, T.J. Yan, J.E. Cavanaugh, P.T. Flaherty, B.S. Beckman, M.E. Burow, Oncogenic signaling of MEK5-ERK5, Cancer Lett. 28 (392) (2017 Apr) 51–59.
[65] Y. Chen, J.Q. Chen, M.M. Ge, Q. Zhang, X.Q. Wang, J.Y. Zhu, et al., Sulforaphane inhibits epithelial-mesenchymal transition by activating extracellular signal-regulated kinase 5 in lung cancer cells, J. Nutr. Biochem. 72 (2019 Oct) 108219.
[66] A.B. Bhatt, S. Patel, M.D. Matossian, D.A. Ucar, L. Miele, M.E. Burow, et al., Molecular mechanisms of epithelial to mesenchymal transition regulated by ERK5 signaling, Biomolecules 11 (2) (2021 Feb) 183.
[67] S.J. Park, Y.S. Choi, S. Lee, Y.J. Lee, S. Hong, S. Han, et al., BIX02189 inhibits TGF-β1-induced lung cancer cell metastasis by directly targeting TGF-β type I receptor, Cancer Lett. 381 (2) (2016 Oct 28) 314–322.
[68] J.C. Barros, C.J. Marshall, Activation of either ERK1/2 or ERK5 MAP kinase pathways can lead to disruption of the actin cytoskeleton, J. Cell Sci. 118 (Pt 8) (2005 Apr 15) 1663–1671.
[69] H. Sheng, J. Shao, M.K. Washington, R.N. DuBois, Prostaglandin E2 increases growth and motility of colorectal carcinoma cells*, J. Biol. Chem. 276 (21) (2001 May 25) 18075–18081.
[70] M.A. Masini, V. Bonetto, M. Manfredi, A. Pastò, E. Barberis, S. Timo, et al., Prolonged exposure to simulated microgravity promotes stemness impairing morphological, metabolic and migratory profile of pancreatic cancer cells: a comprehensive proteomic, lipidomic and trans- criptomic analysis, Cell. Mol. Life Sci. 79 (5) (2022 Apr 7) 226.
[71] D.M. Pereira, S.E. Gomes, P.M. Borralho, C.M.P. Rodrigues, MEK5/ERK5 activation regulates colon cancer stem-like cell properties, Cell Death Discov. 5 (1) (2019 Feb 11) 1–13.
[72] C.A.C. Williams, R. Fernandez-Alonso, J. Wang, R. Toth, N.S. Gray, G.M. Findlay, Erk5 is a key regulator of naive-primed transition and embryonic stem cell identity, Cell Rep. 16 (7) (2016 Aug 16) 1820–1828.
[73] K. Fukasawa, J. Lyu, T. Kubo, Y. Tanaka, A. Suzuki, T. Horie, et al., MEK5-ERK5 axis promotes self-renewal and tumorigenicity of glioma stem cells, Cancer Res. Commun. 3 (1) (2023 Jan) 148–159.
[74] L. Bazzani, S. Donnini, A. Giachetti, G. Christofori, M. Ziche, PGE 2 mediates EGFR internalization and nuclear translocation via caveolin endocytosis promoting its transcriptional activity and proliferation in human NSCLC cells, Oncotarget 9 (19) (2018 Mar 13) 14939–14958.
[75] S. He, D. Dong, J. Lin, B. Wu, X. Nie, G. Cai, Overexpression of TRAF4 promotes lung cancer growth and EGFR-dependent phosphorylation of ERK5, FEBS Open Bio 12 (10) (2022 Oct) 1747–1760.
[76] W. Zhao, D. Yu, Z. Chen, W. Yao, J. Yang, S.S. Ramalingam, et al., Inhibition of MEK5/ERK5 signaling overcomes acquired resistance to the third generation EGFR inhibitor, osimertinib, via enhancing Bim-dependent apoptosis, Cancer Lett. 28 (519) (2021 Oct) 141–149.